ISSN 2306-5478

УДК 624.012.45 https://doi.org/10.31713/vt2202624

Stoyanovych V.M., ([1])
PhD student
Martyniuk P.M., ([1:ORCID: 0000-0002-2750-2508])
D.Sc. (Engineering), Professor
Kochkarev D.V., ([1:ORCID: 0000-0002-4525-7315])
D.Sc. (Engineering), Professor

[1] National University of Water and Environmental Engineering, Rivne

A PHYSICALLY BASED ANALYTICAL METHOD FOR DETERMINING BLAST-INDUCED ACCELERATION TIME HISTORIES FROM THE ACOUSTIC IMPEDANCE OF THE MEDIUM

This paper presents a physically based analytical approach for determining blast-induced acceleration time histories, which is developed by establishing the relationship between the time-dependent overpressure of a blast wave and the kinematic parameters of particle motion in the surrounding medium. The relevance of the study is associated with the need to obtain reliable acceleration time histories for the dynamic analysis of building structures subjected to impulsive blast loading. Existing design approaches generally provide the main parameters of a blast wave, including peak overpressure, specific impulse, and positive phase duration; however, the determination of acceleration time histories often requires additional assumptions or complex numerical simulations.

The proposed method is based on the one-dimensional wave propagation model in a homogeneous elastic medium and the concept of acoustic impedance. Using the relations of wave theory, a correlation between blast overpressure and particle velocity is derived, which enables the determination of particle velocity from a known pressure–time function. Further differentiation of the obtained relationship provides a direct procedure for calculating the acceleration time history induced by blast loading. The proposed mathematical formulation is universal and can be applied to various pressure–time functions describing blast wave propagation. The practical application of the developed approach is demonstrated using two commonly adopted blast impulse models: a linearly decaying

triangular pressure pulse and the exponential Friedlander waveform. The characteristics of the resulting acceleration time histories are analyzed, and the influence of the pressure-time function shape on acceleration response is evaluated. It is shown that the triangular pulse model produces an acceleration history with an approximately constant acceleration level during the positive phase of the impulse, whereas the Friedlander function results in a gradually decaying acceleration response that more accurately represents the physical attenuation of a blast wave. The analysis demonstrates that the acceleration response is governed not only by the peak overpressure but also by the rate of pressure variation and the duration of the positive phase of the blast pulse. This confirms the importance of considering the temporal structure of blast loading when evaluating the dynamic response of structural systems. The proposed approach is characterized by a clear physical interpretation, computational efficiency, and ease of implementation, making it suitable as an intermediate procedure between blast wave parameter determination and dynamic structural analysis.

The obtained results can be applied for generating design acceleration time histories for time-domain and spectral analyses of structures, as well as for improving methodologies used to assess the load-bearing capacity and structural performance of buildings and protective structures subjected to blast effects.

Key words: blast wave, acceleration time history, acoustic impedance, overpressure, particle velocity, Friedlander waveform, dynamic analysis, impulsive loading.

Review of previous studies and problem statement. A key step in assessing the dynamic effects of blast loading on building structures is obtaining an acceleration time history of ground or foundation motion. Such a record describes particle acceleration as a function of time and is used in direct time integration of the equations of motion, in response-spectrum analysis, and in numerical modelling of structural response. The preferred method for constructing the acceleration time history depends on the required accuracy, the available input data, the complexity of the problem, and the computational resources. Analytical, spectral, numerical, and experimental approaches are all used to obtain blast-induced acceleration time histories, each with its own advantages, limitations, and scope of application. The main approaches are summarised below.

 ISSN 2306-5478

1. Analytical methods based on one-dimensional wave theory [1,2,3];
2. Spectral methods based on the Fourier transform [4, 5];
3. Finite-element numerical modelling in modern analysis software [6,7,8];
4. Semi-empirical scaling of measured acceleration time histories [9, 10];
5. Direct field measurements [11, 12];
6. Differentiation of measured particle-velocity records [13, 14].

Analytical methods based on one-dimensional wave theory treat blast-wave propagation in a one-dimensional medium and use acoustic impedance to relate overpressure to particle velocity. Once a pressure–time history is prescribed (for example, a triangular pulse or a Friedlander waveform), the acceleration time history follows by differentiating velocity with respect to time. This approach is used in engineering practice and underpins UFC guidance [1] on medium motion under blast loading. It has a clear physical basis, is straightforward to implement, and requires little computational effort, so acceleration time histories can be generated quickly for different pressure–time laws. Its principal limitation is the assumption of one-dimensional propagation, which means that complex geometry, soil heterogeneity, reflections, and wave interference are not fully captured.

Spectral methods based on the Fourier transform convert a time-domain signal into the frequency domain using the fast Fourier transform (FFT). After the spectrum of velocity or pressure has been obtained, acceleration is recovered by multiplying each harmonic component by the corresponding circular frequency and applying the inverse transform. The method is widely used to process experimental blast records: it accommodates arbitrary signal shapes, provides spectral content, and supports digital filtering. It is computationally efficient and integrates readily with modern signal-processing tools. However, it does not describe the physics of blast-wave propagation and requires a measured or otherwise prescribed input signal; the results also depend on the sampling rate and may be affected by edge effects.

Finite-element numerical modelling solves the governing equations of continuum dynamics using modern software packages (e.g., LS-DYNA, Abaqus Explicit, AUTODYN). Shock-wave propagation, soil–structure interaction, material nonlinearity, contact, and possible structural failure can be treated within a single analysis, and the acceleration time history is obtained from nodal accelerations. This

approach offers the highest fidelity and can represent realistic geometry, heterogeneous soils, complex wave fields, and nonlinear material response; it is therefore the most versatile option for demanding problems. Model development, however, is time-consuming and computationally expensive, and requires detailed material data. Result quality depends strongly on the chosen constitutive models and analysis settings.

Semi-empirical methods start from measured acceleration time histories and scale them with charge mass, standoff distance, and medium properties. Their strength is that they retain features of real blast-wave propagation; their use is limited by the available experimental database and by how closely the test conditions match the design case.

Direct field measurements record acceleration during full-scale blast tests using accelerometers or geophones. Such records are the most reliable observational data, but the tests are costly and logistically demanding, and the amount of published data remains limited.

Acceleration time histories can also be obtained by numerical differentiation of measured particle-velocity records. The procedure is simple and common in geophysical data processing, but it amplifies noise and therefore requires prior digital filtering.

Overall, existing methods for obtaining blast-induced acceleration time histories are either computationally demanding or dependent on experimental records. Design documents such as UFC [1] emphasise blast-wave parameters, while procedures for converting those parameters into acceleration time histories for structural analysis remain comparatively underdeveloped. This motivates a simple, physically based analytical method that yields acceleration time histories directly from known blast loading parameters.

The objective of this study is to develop such a method from the relationship between blast-wave pressure and particle velocity, using the acoustic impedance of the medium. Specifically, we:

- derive an analytical relationship between blast-wave overpressure and particle velocity;
- obtain a general expression for the acceleration time history by differentiating the velocity history;
- develop closed-form acceleration time histories for the most common pressure–time models (a triangular pulse and the Friedlander waveform).

 ISSN 2306-5478

Proposed method.

Construction of the blast-induced acceleration time history begins with the particle-velocity history. Consider a plane shock wave propagating in a homogeneous medium, and adopt the wave-theory relations that link overpressure to particle velocity.

Figure 1 shows an infinitesimal continuum (soil) element of length dx, with stresses acting on the left face at σ(x) and on the right face at σ(x+dx).

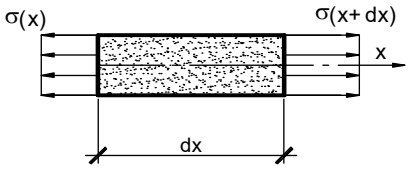


Figure 1. Derivation of Newton's second law in impulse form for one-dimensional continuum waves

The resultant force F on the element is obtained by projecting all forces onto the x-axis:

$$F = \sigma(x + dx) - \sigma(x). \quad (1)$$

Expanding the first term of Eq. (1) in a Taylor series gives

$$\sigma(x + dx) \approx \sigma(x) + \frac{\partial \sigma}{\partial x} dx. \quad (2)$$

Substituting Eq. (2) into Eq. (1) and simplifying yields

$$F = \frac{\partial \sigma}{\partial x} dx. \quad (3)$$

The mass of the infinitesimal element is

$$m = \rho \cdot dx, \quad (4)$$

where ρ denotes the linear density of the material.

If u is the particle displacement, acceleration is the second time derivative of displacement:

$$a(t) = \frac{\partial^2 u}{\partial t^2}. \quad (5)$$

Newton's second law applied to the element in Fig. 1 then gives

$$F = m \cdot a. \quad (6)$$

Substitution of Eqs. (3)–(5) into Eq. (6) produces

$$\frac{\partial \sigma}{\partial x} dx = \rho dx \frac{\partial^2 u}{\partial t^2}. \quad (7)$$

Cancelling dx in Eq. (7) leads to the governing equation of motion

$$\frac{\partial \sigma}{\partial x} = \rho \frac{\partial^2 u}{\partial t^2}. \quad (8)$$

Particle velocity v is the first time derivative of displacement:

$$v = \frac{\partial u}{\partial t}. \tag{9}$$

Expressing the momentum balance (8) in terms of velocity via Eq. (9) gives

$$\frac{\partial \sigma}{\partial x} = \rho \frac{\partial v}{\partial t}. \tag{10}$$

Invoking Hooke's law, the stress may be written as

$$\sigma = E \cdot \varepsilon = E \frac{\partial u}{\partial x}, \tag{11}$$

where E is the elastic modulus along the element. Substituting Eq. (11) into Eq. (8) recovers the classical wave equation

$$\frac{\partial^2 u}{\partial t^2} = \frac{E}{\rho} \frac{\partial^2 u}{\partial x^2}. \tag{12}$$

Introducing the notation

$$c = \sqrt{\frac{E}{\rho}} \Rightarrow E = \rho c^2, \tag{13}$$

where c is the longitudinal wave speed in the soil.

Equation (12) may then be written as

$$\frac{\partial^2 u}{\partial t^2} = c^2 \frac{\partial^2 u}{\partial x^2}. \tag{14}$$

A solution of Eq. (14) is sought in the form of a travelling wave whose shape is preserved as it propagates. Introducing the characteristic variable [15]

$$\xi = x - ct. \tag{15}$$

the displacement may be written as

$$u(x,t) = f(\xi). \tag{16}$$

Differentiating with respect to time once gives

$$\frac{\partial u}{\partial t} = \frac{\partial f(\xi)}{\partial \xi} \frac{\partial \xi}{\partial t}, \quad \frac{\partial \xi}{\partial t} = \frac{\partial (x - ct)}{\partial t} = -c \Rightarrow \frac{\partial u}{\partial t} = -c \frac{\partial f(\xi)}{\partial \xi}. \tag{17}$$

and a second differentiation yields

$$\frac{\partial^2 u}{\partial t^2} = -c \frac{\partial}{\partial t}\left(\frac{\partial f(\xi)}{\partial \xi} \frac{\partial \xi}{\partial t} \right), \quad \frac{\partial \xi}{\partial t} = \frac{\partial (x - ct)}{\partial t} = -c \Rightarrow \frac{\partial^2 u}{\partial t^2} = c^2 \frac{\partial f^2(\xi)}{\partial \xi^2}. \tag{18}$$

The first spatial derivative is

$$\frac{\partial u}{\partial x} = \frac{\partial f(\xi)}{\partial \xi} \frac{\partial \xi}{\partial x}, \quad \frac{\partial \xi}{\partial x} = \frac{\partial (x - ct)}{\partial x} = 1 \Rightarrow \frac{\partial u}{\partial x} = \frac{\partial f(\xi)}{\partial \xi}. \tag{19}$$

and the second spatial derivative is

 ISSN 2306-5478

$$\frac{\partial^2 u}{\partial x^2} = \frac{\partial}{\partial x}\left(\frac{\partial f(\xi)}{\partial \xi}\frac{\partial \xi}{\partial x}\right), \quad \frac{\partial \xi}{\partial x} = \frac{\partial (x - ct)}{\partial x} = 1 \Rightarrow \frac{\partial^2 u}{\partial t^2} = \frac{\partial f^2(\xi)}{\partial \xi^2}. \quad (20)$$

Substitution of Eqs. (18) and (20) into Eq. (14) produces an identity

$$c^2 \frac{\partial f^2(\xi)}{\partial \xi^2} = c^2 \frac{\partial f^2(\xi)}{\partial \xi^2}. \quad (21)$$

Hence any twice differentiable function of (x – ct) satisfies Eq. (14).

For unidirectional plane waves, the solution of Eq. (14) therefore takes the form

$$u = f(x - ct). \quad (22)$$

With the characteristic coordinates ξ = x – ct and η = x + ct, the general solution becomes

$$u = f(x - ct) + g(x + ct). \quad (23)$$

and the wave equation reduces to the canonical form

$$\frac{\partial^2 u}{\partial \xi \partial \eta} = 0. \quad (24)$$

In this form, variations associated with one characteristic direction are independent of those associated with the other. The same separation of incident and reflected impulses is adopted in UFC [1].

For the plane waves considered here, particle velocity and strain are

$$v = \frac{\partial u}{\partial t} = -c \cdot \frac{\partial f(x - ct)}{\partial (x - ct)}; \quad (25)$$

$$\varepsilon = \frac{\partial u}{\partial x} = \frac{\partial f(x - ct)}{\partial (x - ct)}. \quad (26)$$

The stress then follows from Eqs. (11) and (26):

$$\sigma = E \frac{\partial f(x - ct)}{\partial (x - ct)} = \rho \cdot c^2 \frac{\partial f(x - ct)}{\partial (x - ct)}. \quad (27)$$

From Eq. (25), the relevant time derivative is

$$\frac{\partial f(x - ct)}{\partial (x - ct)} = -\frac{v}{c}. \quad (28)$$

Substituting Eq. (28) into Eq. (27) and rearranging gives the pressure–velocity relation

$$\sigma = \rho \cdot c^2 \left(-\frac{v}{c}\right) = -\rho \cdot c \cdot v. \quad (29)$$

Thus, under the assumptions adopted for a homogeneous medium, the kinematic response of the soil follows directly from the overpressure history P(t) at the wave front and the particle velocity V(t):

$$V(t) = \frac{P(t)}{\rho \cdot C_V}, \tag{30}$$

where ρ is the soil density and Cv is the wave speed in the soil.

Equation (30) determines particle velocity from a known overpressure–time history. Because acceleration is the time derivative of velocity, the acceleration time history is

$$a(t) = \frac{dV(t)}{dt}. \tag{31}$$

Substitution of Eq. (30) then yields the general expression

$$a_V = \frac{dV(t)}{dt} = \frac{1}{\rho C_V}\frac{dP(t)}{dt}. \tag{32}$$

Equation (32) is now specialised to two representative pressure–time functions.

First, consider a linearly decaying triangular pressure pulse

$$P(t) = P_{max} \cdot \left(1 - \frac{t}{t_0}\right), 0 \le t \le t_0, \tag{33}$$

where P_{max} is the peak pressure, expressed as a function of the scaled distance $Z = R/W^{1/3}$ (R is the distance from the charge centre to the point of interest and W is the TNT-equivalent charge mass), and t_0 is the positive-phase duration. The corresponding particle velocity is

$$V(t) = \frac{P_{max}}{\rho C_v}\left(1 - \frac{t}{t_0}\right). \tag{34}$$

and the acceleration time history reduces to

$$a_V = \frac{dV_V(t)}{dt} = \frac{1}{\rho C_V}\frac{dP(t)}{dt} = -\frac{P_{max}}{\rho C_V t_0}. \tag{35}$$

UFC [1] recommends the simplified expression (35) with a constant load duration for all explosion types considered therein:

$$a_V = 100\frac{P_{max}}{\rho C_V}. \tag{36}$$

A more realistic acceleration time history is obtained when the pressure history is described by the exponential Friedlander waveform

$$P(t) = P_{max} \cdot \left(1 - \frac{t}{t_0}\right) \cdot e^{-b\frac{t}{t_0}}, \tag{37}$$

where P_{max} depends on the scaled distance Z, t_0 is the positive-phase duration, and b is the waveform decay parameter. Restricting attention

 ISSN 2306-5478

to the compressive phase, differentiation of Eq. (37) gives the acceleration time history

$$a_V = \frac{dV_V(t)}{dt} = \frac{1}{\rho C_V}\frac{dP(t)}{dt} = \frac{P_{max}}{\rho C_V t_0} e^{-b\frac{t}{t_0}}\left(\frac{b\cdot t}{t_0} - b - 1\right), \quad (38)$$

The time at which the acceleration decreases to zero is determined by

$$\left(\frac{b\cdot t}{t_0} - b - 1\right) = 0 \rightarrow \; t = t_0\frac{(b+1)}{b}. \quad (39)$$

The shape of the resulting acceleration time histories is controlled by the prescribed pressure–time history. For the triangular pulse, linear pressure decay produces a rectangular acceleration history with constant amplitude during the positive phase. This idealisation is convenient for engineering estimates but does not capture the true decay of a blast wave. The Friedlander waveform yields a decaying acceleration history that is more consistent with shock-wave attenuation. Peak acceleration depends not only on peak pressure but also on the rate of pressure change. Accordingly, the Friedlander representation is preferable when accounting for the realistic profile (or actual shape) of the blast impulse is required.

Conclusions.

A physically based analytical method has been developed for constructing blast-induced acceleration time histories from blast-wave parameters and the kinematic response of the surrounding medium. Using a one-dimensional wave model and acoustic impedance, overpressure is related to particle velocity, and acceleration is obtained by differentiating the pressure–time history. The approach is independent of any particular impulse shape: both a linearly decaying triangular pulse and a Friedlander waveform yield closed-form acceleration time histories without recourse to detailed numerical simulation.

The acceleration time history is governed not only by peak overpressure but also by the temporal evolution of pressure. For a given peak pressure, changes in impulse duration can produce substantially different accelerations, which should be accounted for in dynamic structural analysis.

The method is physically transparent, easy to implement, and compatible with existing procedures for the dynamic analysis of building structures. It can be used to generate design acceleration time

histories for blast assessment and provides an intermediate step between evaluation of blast-wave parameters and calculation of the structural response.

1. Unified Facilities Criteria. UFC 3-340-02 Structures to Resist the Effects of Accidental Explosions. Washington: U.S. Army Corps of Engineers, Naval Facilities Engineering Command, Air Force Civil Engineer Support Agency, 2008. 2. Kochkarev, D., Azizov, T., &Galinska, T. (2024). Calculation of Buildings and Structures for Air Blasts Using Explosion Accelerograms. Proceedings of EcoComfort 2024, 245–256. https://doi.org/10.1007/978-3-031-67576-8_22. 3. Aftabi, Milad, Motamedi, Mohammad hossein, Molladavoodi, Hamed, A Study on Parameters Influencing Blast-Induced Frequency Content and Dominant Frequency Attenuation, Shock and Vibration, 2022, 4626536, 11 pages, 2022. https://doi.org/10.1155/2022/4626536 4. Michael Saleh, Lyndon Edwards, Evaluation of soil and fluid structure interaction in blast modelling of the flying plate test, Computers & Structures, Volume 151, 2015, Pages 96-114, ISSN 0045-7949, https://doi.org/10.1016/j.compstruc.2015.01.010.
5. Biessikirski, A., Jakóbczyk, J. Application of strain gauge and geophone based integrated monitoring system in the measurements of the blast induced low-frequency vibrations. Sci Rep 15, 9544 (2025). https://doi.org/10.1038/s41598-025-94128-5 6. Sun, Y., Zhang, Z., Tian, C. et al. Analysis and application of PPV vibration reduction technology in subgrade step blasting - a case study. Sci Rep 15, 17859 (2025). https://doi.org/10.1038/s41598-025-02269-4. 7. Choi, Y.-H.; Lee, S.S. Predictive Modelling for Blasting-Induced Vibrations from Open-Pit Excavations. Appl. Sci. 2021, 11, 7487. https://doi.org/10.3390/app11167487 8. Abebe, S., & Mohammed, T. A. (2022). Performance Assessment of Reinforced Concrete Frame under Close-In Blast Loading. Advances in Civil Engineering, 2022, 3979195. https://doi.org/10.1155/2022/3979195 9. Shi, Y., Hao, H. & Li, ZX. Numerical simulation of blast wave interaction with structure columns. Shock Waves 17, 113–133 (2007). https://doi.org/10.1007/s00193-007-0099-5 10. Ranjan Kumar, Deepankar Choudhury, Kapilesh Bhargava, Determination of blast-induced ground vibration equations for rocks using mechanical and geological properties, Journal of Rock Mechanics and Geotechnical Engineering, Volume 8, Issue 3, 2016, Pages 341-349, ISSN 1674-7755, https://doi.org/10.1016/j.jrmge.2015.10.009. 11. Al-Qasimi, E. M. A., W. A. Charlie, and D. J. Woeller. 2005. “Canadian liquefaction experiment (CANLEX): Blast-induced ground motion and pore pressure experiments.” Geotech. Test. J. 28 (1): 9–21. https://doi.org/10.1520/GTJ11848. 12. Agrawal, H., and A. K. Mishra. 2019. “Modified scaled distance regression analysis approach for prediction of blast-induced ground vibration in multi-hole blasting.” J. Rock Mech. Geotech. Eng. 11 (1): 202–207.

ISSN 2306-5478

https://doi.org/10.1016/j.jrmge.2018.07.004. 13. Sun, Y., Zhang, Z., Tian, C. et al. Analysis and application of PPV vibration reduction technology in subgrade step blasting - a case study. Sci Rep 15, 17859 (2025). https://doi.org/10.1038/s41598-025-02269-4. 14. Guo, J.; Fei, H.; Yan, Y. Research and Advances in the Characteristics of Blast-Induced Vibration Frequencies. Buildings 2025, 15, 892. https://doi.org/10.3390/15060892. 15. Pinchover, Y.; Rubinstein, J. An Introduction to Partial Differential Equations; Cambridge University Press: Cambridge, UK, 2005. ISBN 978-0-521-61323-1.

REFERENCES:

1. Unified Facilities Criteria. UFC 3-340-02 Structures to Resist the Effects of Accidental Explosions. Washington: U.S. Army Corps of Engineers, Naval Facilities Engineering Command, Air Force Civil Engineer Support Agency, 2008. 2. Kochkarev, D., Azizov, T., &Galinska, T. (2024). Calculation of Buildings and Structures for Air Blasts Using Explosion Accelerograms. Proceedings of EcoComfort 2024, 245–256. https://doi.org/10.1007/978-3-031-67576-8_22. 3. Aftabi, Milad, Motamedi, Mohammad hossein, Molladavoodi, Hamed, A Study on Parameters Influencing Blast-Induced Frequency Content and Dominant Frequency Attenuation, Shock and Vibration, 2022, 4626536, 11 pages, 2022. https://doi.org/10.1155/2022/4626536 4. Michael Saleh, Lyndon Edwards, Evaluation of soil and fluid structure interaction in blast modelling of the flying plate test, Computers & Structures, Volume 151, 2015, Pages 96-114, ISSN 0045-7949, https://doi.org/10.1016/j.compstruc.2015.01.010.
5. Biessikirski, A., Jakóbczyk, J. Application of strain gauge and geophone based integrated monitoring system in the measurements of the blast induced low-frequency vibrations. Sci Rep 15, 9544 (2025). https://doi.org/10.1038/s41598-025-94128-5 6. Sun, Y., Zhang, Z., Tian, C. et al. Analysis and application of PPV vibration reduction technology in subgrade step blasting - a case study. Sci Rep 15, 17859 (2025). https://doi.org/10.1038/s41598-025-02269-4. 7. Choi, Y.-H.; Lee, S.S. Predictive Modelling for Blasting-Induced Vibrations from Open-Pit Excavations. Appl. Sci. 2021, 11, 7487. https://doi.org/10.3390/app11167487 8. Abebe, S., & Mohammed, T. A. (2022). Performance Assessment of Reinforced Concrete Frame under Close-In Blast Loading. Advances in Civil Engineering, 2022, 3979195. https://doi.org/10.1155/2022/3979195 9. Shi, Y., Hao, H. & Li, ZX. Numerical simulation of blast wave interaction with structure columns. Shock Waves 17, 113–133 (2007). https://doi.org/10.1007/s00193-007-0099-5 10. Ranjan Kumar, Deepankar Choudhury, Kapilesh Bhargava, Determination of blast-induced ground vibration equations for rocks using mechanical and geological properties, Journal of Rock Mechanics and Geotechnical Engineering, Volume 8, Issue 3, 2016, Pages 341-349, ISSN 1674-7755, https://doi.org/10.1016/j.jrmge.2015.10.009. 11. Al-Qasimi, E. M. A., W. A.

Charlie, and D. J. Woeller. 2005. “Canadian liquefaction experiment (CANLEX): Blast-induced ground motion and pore pressure experiments.” Geotech. Test. J. 28 (1): 9–21. https://doi.org/10.1520/GTJ11848. 12. Agrawal, H., and A. K. Mishra. 2019. “Modified scaled distance regression analysis approach for prediction of blast-induced ground vibration in multi-hole blasting.” J. Rock Mech. Geotech. Eng. 11 (1): 202–207. https://doi.org/10.1016/j.jrmge.2018.07.004. 13. Sun, Y., Zhang, Z., Tian, C. et al. Analysis and application of PPV vibration reduction technology in subgrade step blasting - a case study. Sci Rep 15, 17859 (2025). https://doi.org/10.1038/s41598-025-02269-4. 14. Guo, J.; Fei, H.; Yan, Y. Research and Advances in the Characteristics of Blast-Induced Vibration Frequencies. Buildings 2025, 15, 892. https://doi.org/10.3390/15060892. 15. Pinchover, Y.; Rubinstein, J. An Introduction to Partial Differential Equations; Cambridge University Press: Cambridge, UK, 2005. ISBN 978-0-521-61323-1.

Стоянович В.М., ([1])
аспірант
Мартинюк П.М., ([1:ORCID: 0000-0002-2750-2508])
д.т.н., проф.
Кочкарьов Д.В., ([1:ORCID: 0000-0002-4525-7315])
д.т.н., проф.

[1] Національний університет водного господарства та природокористування, м. Рівне

ФІЗИЧНО ОБҐРУНТОВАНИЙ АНАЛІТИЧНИЙ МЕТОД ВИЗНАЧЕННЯ АКСЕЛЕРОГРАМ ВИБУХОВОГО НАВАНТАЖЕННЯ НА ОСНОВІ АКУСТИЧНОГО ІМПЕДАНСУ СЕРЕДОВИЩА

У статті представлено фізично обґрунтований аналітичний метод визначення акселерограм вибухового навантаження на основі взаємозв’язку між надлишковим тиском ударної хвилі та швидкістю руху частинок середовища. Запропонований підхід базується на одномірній хвильовій моделі та використанні акустичного імпедансу, що дозволяє отримати часову залежність прискорення без проведення складного чисельного моделювання. Виведено залежність для визначення акселерограми через похідну функції тиску в часі. Розглянуто застосування запропонованої методики для найбільш поширених моделей вибухового імпульсу: спадного трикутного імпульсу та функції Фрідлендера. Проведено

ISSN 2306-5478

аналіз впливу форми імпульсу на характер зміни прискорення. Встановлено, що величина акселерограми визначається не тільки максимальним тиском, але й швидкістю його зміни у часі. Запропонована методика може бути використана для динамічного розрахунку будівельних конструкцій за дії вибухових навантажень. Отримані залежності дозволяють формувати розрахункові акселерограми безпосередньо за параметрами вибухової хвилі, які визначаються існуючими нормативними методами. Результати дослідження створюють основу для подальшого використання запропонованого підходу у спектральних та часових методах розрахунку споруд на дію імпульсних вибухових навантажень.
Ключові слова: вибухова хвиля, акселерограма, акустичний імпеданс, надлишковий тиск, функція Фрідлендера, динамічний розрахунок.

Отримано: 29 березня 2026 року
Прорецензовано: 25 квітня 2026 року
Прийнято до друку: 29 травня 2026 року

© 2026 [Stoyanovych V.M., Martyniuk P.M., Kochkarev D.V.]. Licensee [NUWEE]. This article is an open access article distributed under the terms and conditions of the Creative Commons Attribution-NonCommercial (CC BY-NC) license (creativecommons.org).